Fermi National Accelerator Laboratory

FERMILAB-Pub-96/071-E
CDF

Forward-Backward Charge Asymmetry of Electron Pairs Above the Z^0 Pole

F. Abe et al.
The CDF Collaboration

Fermi National Accelerator Laboratory
P.O. Box 500, Batavia, Illinois 60510

March 1996

Submitted to *Physical Review Letters*

Operated by Universities Research Association Inc. under Contract No. DE-AC02-76CHO3000 with the United States Department of Energy

Disclaimer

This report was prepared as an account of work sponsored by an agency of the United States Government. Neither the United States Government nor any agency thereof, nor any of their employees, makes any warranty, expressed or implied, or assumes any legal liability or responsibility for the accuracy, completeness, or usefulness of any information, apparatus, product, or process disclosed, or represents that its use would not infringe privately owned rights. Reference herein to any specific commercial product, process, or service by trade name, trademark, manufacturer, or otherwise, does not necessarily constitute or imply its endorsement, recommendation, or favoring by the United States Government or any agency thereof. The views and opinions of authors expressed herein do not necessarily state or reflect those of the United States Government or any agency thereof.

CDF/PUB/ELECTROWEAK/CDFR/3493

Forward-Backward Charge Asymmetry of Electron Pairs Above the Z^0 Pole

F. Abe,[14] H. Akimoto,[32] A. Akopian,[27] M. G. Albrow,[7] S. R. Amendolia,[24] D. Amidei,[17] J. Antos,[29] C. Anway-Wiese,[4] S. Aota,[32] G. Apollinari,[27] T. Asakawa,[32] W. Ashmanskas,[15] M. Atac,[7] P. Auchincloss,[26] F. Azfar,[22] P. Azzi-Bacchetta,[21] N. Bacchetta,[21] W. Badgett,[17] S. Bagdasarov,[27] M. W. Bailey,[19] J. Bao,[35] P. de Barbaro,[26] A. Barbaro-Galtieri,[15] V. E. Barnes,[25] B. A. Barnett,[13] P. Bartalini,[24] G. Bauer,[16] T. Baumann,[9] F. Bedeschi,[24] S. Behrends,[3] S. Belforte,[24] G. Bellettini,[24] J. Bellinger,[34] D. Benjamin,[31] J. Benlloch,[16] J. Bensinger,[3] D. Benton,[22] A. Beretvas,[7] J. P. Berge,[7] J. Berryhill,[5] S. Bertolucci,[8] A. Bhatti,[27] K. Biery,[12] M. Binkley,[7] D. Bisello,[21] R. E. Blair,[1] C. Blocker,[3] A. Bodek,[26] W. Bokhari,[16] V. Bolognesi,[24] D. Bortoletto,[25] J. Boudreau,[23] G. Brandenburg,[9] L. Breccia,[2] C. Bromberg,[18] E. Buckley-Geer,[7] H. S. Budd,[26] K. Burkett,[17] G. Busetto,[21] A. Byon-Wagner,[7] K. L. Byrum,[1] J. Cammerata,[13] C. Campagnari,[7] M. Campbell,[17] A. Caner,[7] W. Carithers,[15] D. Carlsmith,[34] A. Castro,[21] D. Cauz,[24] Y. Cen,[26] F. Cervelli,[24] H. Y. Chao,[29] J. Chapman,[17] M.-T. Cheng,[29] G. Chiarelli,[24] T. Chikamatsu,[32] C. N. Chiou,[29] L. Christofek,[11] S. Cihangir,[7] A. G. Clark,[24] M. Cobal,[24] M. Contreras,[5] J. Conway,[28] J. Cooper,[7] M. Cordelli,[8] C. Couyoumtzelis,[24] D. Crane,[1] D. Cronin-Hennessy,[6] R. Culbertson,[5] J. D. Cunningham,[3] T. Daniels,[16] F. DeJongh,[7] S. Delchamps,[7] S. Dell'Agnello,[24] M. Dell'Orso,[24] L. Demortier,[27] B. Denby,[24] M. Deninno,[2] P. F. Derwent,[17] T. Devlin,[28] M. Dickson,[26] J. R. Dittmann,[6] S. Donati,[24] R. B. Drucker,[15] A. Dunn,[17] N. Eddy,[17] K. Einsweiler,[15] J. E. Elias,[7] R. Ely,[15] E. Engels, Jr.,[23] D. Errede,[11] S. Errede,[11] Q. Fan,[26] I. Fiori,[2] B. Flaugher,[7] G. W. Foster,[7] M. Franklin,[9] M. Frautschi,[19] J. Freeman,[7] J. Friedman,[16] H. Frisch,[5] T. A. Fuess,[1] Y. Fukui,[14] S. Funaki,[32] G. Gagliardi,[24] S. Galeotti,[24] M. Gallinaro,[21] M. Garcia-Sciveres,[15] A. F. Garfinkel,[25] C. Gay,[9] S. Geer,[7] D. W. Gerdes,[17] P. Giannetti,[24] N. Giokaris,[27] P. Giromini,[8] L. Gladney,[22] D. Glenzinski,[13] M. Gold,[19] J. Gonzalez,[22] A. Gordon,[9] A. T. Goshaw,[6] K. Goulianos,[27] H. Grassmann,[7a] L. Groer,[28] C. Grosso-Pilcher,[5] G. Guillian,[17] R. S. Guo,[29] C. Haber,[15] S. R. Hahn,[7] R. Hamilton,[9] R. Handler,[34] R. M. Hans,[35] K. Hara,[32] B. Harral,[22] R. M. Harris,[7] S. A. Hauger,[6] J. Hauser,[4] C. Hawk,[28] E. Hayashi,[32] J. Heinrich,[22] M. Hohlmann,[1,5] C. Holck,[22] R. Hollebeek,[22] L. Holloway,[11] A. Hölscher,[12] S. Hong,[17] G. Houk,[22] P. Hu,[23] B. T. Huffman,[23] R. Hughes,[26] J. Huston,[18] J. Huth,[9] J. Hylen,[7] H. Ikeda,[32] M. Incagli,[24] J. Incandela,[7] J. Iwai,[32] Y. Iwata,[10] H. Jensen,[7] U. Joshi,[7] R. W. Kadel,[15] E. Kajfasz,[7a] T. Kamon,[30] T. Kaneko,[32] K. Karr,[33] H. Kasha,[35] Y. Kato,[20] L. Keeble,[8] K. Kelley,[16] R. D. Kennedy,[28] R. Kephart,[7] P. Kesten,[15] D. Kestenbaum,[9] R. M. Keup,[11] H. Keutelian,[7] F. Keyvan,[4] B. J. Kim,[26] D. H. Kim,[7a] H. S. Kim,[12] S. B. Kim,[17] S. H. Kim,[32] Y. K. Kim,[15] L. Kirsch,[3] P. Koehn,[26] K. Kondo,[32] J. Konigsberg,[9] S. Kopp,[5] K. Kordas,[12] W. Koska,[7] E. Kovacs,[7a] W. Kowald,[6] M. Krasberg,[17] J. Kroll,[7] M. Kruse,[25] T. Kuwabara,[32] S. E. Kuhlmann,[1] E. Kuns,[28] A. T. Laasanen,[25] N. Labanca,[24] S. Lammel,[7] J. I. Lamoureux,[3] T. LeCompte,[11] S. Leone,[24] J. D. Lewis,[7] P. Limon,[7] M. Lindgren,[4] T. M. Liss,[11] N. Lockyer,[22] O. Long,[22] C. Loomis,[28] M. Loreti,[21] J. Lu,[30]

D. Lucchesi,[24] P. Lukens,[7] S. Lusin,[34] J. Lys,[15] K. Maeshima,[7] A. Maghakian,[27] P. Maksimovic,[16] M. Mangano,[24] J. Mansour,[18] M. Mariotti,[21] J. P. Marriner,[7] A. Martin,[11] J. A. J. Matthews,[19] R. Mattingly,[16] P. McIntyre,[30] P. Melese,[27] A. Menzione,[24] E. Meschi,[24] S. Metzler,[22] C. Miao,[17] G. Michail,[9] S. Mikamo,[14] R. Miller,[18] H. Minato,[32] S. Miscetti,[8] M. Mishina,[14] H. Mitsushio,[32] T. Miyamoto,[32] S. Miyashita,[32] Y. Morita,[14] J. Mueller,[23] A. Mukherjee,[7] T. Muller,[4] P. Murat,[24] H. Nakada,[32] I. Nakano,[32] C. Nelson,[7] D. Neuberger,[4] C. Newman-Holmes,[7] M. Ninomiya,[32] L. Nodulman,[1] S. Ogawa,[32] S. H. Oh,[6] K. E. Ohl,[35] T. Ohmoto,[10] T. Ohsugi,[10] R. Oishi,[32] M. Okabe,[32] T. Okusawa,[20] R. Oliver,[22] J. Olsen,[34] C. Pagliarone,[2] R. Paoletti,[24] V. Papadimitriou,[31] S. P. Pappas,[35] S. Park,[7] J. Patrick,[7] G. Pauletta,[24] M. Paulini,[15] L. Pescara,[21] M. D. Peters,[15] T. J. Phillips,[6] G. Piacentino,[2] M. Pillai,[26] K. T. Pitts,[7] R. Plunkett,[7] L. Pondrom,[34] J. Proudfoot,[1] F. Ptohos,[9] G. Punzi,[24] K. Ragan,[12] A. Ribon,[21] F. Rimondi,[2] L. Ristori,[24] W. J. Robertson,[6] T. Rodrigo,[7a] J. Romano,[5] L. Rosenson,[16] R. Roser,[11] W. K. Sakumoto,[26] D. Saltzberg,[5] A. Sansoni,[8] L. Santi,[24] H. Sato,[32] V. Scarpine,[30] P. Schlabach,[9] E. E. Schmidt,[7] M. P. Schmidt,[35] G. F. Sciacca,[24] A. Scribano,[24] S. Segler,[7] S. Seidel,[19] Y. Seiya,[32] G. Sganos,[12] A. Sgolacchia,[2] M. D. Shapiro,[15] N. M. Shaw,[25] Q. Shen,[25] P. F. Shepard,[23] M. Shimojima,[32] M. Shochet,[5] J. Siegrist,[15] A. Sill,[31] P. Sinervo,[12] P. Singh,[23] J. Skarha,[13] K. Sliwa,[33] D. A. Smith,[24] F. D. Snider,[13] T. Song,[17] J. Spalding,[7] P. Sphicas,[16] L. Spiegel,[7] A. Spies,[13] L. Stanco,[21] J. Steele,[34] A. Stefanini,[24] K. Strahl,[12] J. Strait,[7] D. Stuart,[7] G. Sullivan,[5] A. Soumarokov,[29] K. Sumorok,[16] J. Suzuki,[32] T. Takada,[32] T. Takahashi,[20] T. Takano,[32] K. Takikawa,[32] N. Tamura,[10] F. Tartarelli,[24] W. Taylor,[12] P. K. Teng,[29] Y. Teramoto,[20] S. Tether,[16] D. Theriot,[7] T. L. Thomas,[19] R. Thun,[17] M. Timko,[33] P. Tipton,[26] A. Titov,[27] S. Tkaczyk,[7] D. Toback,[5] K. Tollefson,[26] A. Tollestrup,[7] J. Tonnison,[25] J. F. de Troconiz,[9] S. Truitt,[17] J. Tseng,[13] N. Turini,[24] T. Uchida,[32] N. Uemura,[32] F. Ukegawa,[22] G. Unal,[22] S. C. van den Brink,[23] S. Vejcik, III,[17] G. Velev,[24] R. Vidal,[7] M. Vondracek,[11] D. Vucinic,[16] R. G. Wagner,[1] R. L. Wagner,[7] J. Wahl,[5] R. C. Walker,[26] C. Wang,[6] C. H. Wang,[29] G. Wang,[24] J. Wang,[5] M. J. Wang,[29] Q. F. Wang,[27] A. Warburton,[12] G. Watts,[26] T. Watts,[28] R. Webb,[30] C. Wei,[6] C. Wendt,[34] H. Wenzel,[15] W. C. Wester, III,[7] A. B. Wicklund,[1] E. Wicklund,[7] R. Wilkinson,[22] H. H. Williams,[22] P. Wilson,[5] B. L. Winer,[26] D. Wolinski,[17] J. Wolinski,[30] X. Wu,[24] J. Wyss,[21] A. Yagil,[7] W. Yao,[15] K. Yasuoka,[32] Y. Ye,[12] G. P. Yeh,[7] P. Yeh,[29] M. Yin,[6] J. Yoh,[7] C. Yosef,[18] T. Yoshida,[20] D. Yovanovitch,[7] I. Yu,[35] J. C. Yun,[7] A. Zanetti,[24] F. Zetti,[24] L. Zhang,[34] W. Zhang,[22] and S. Zucchelli[2]

(CDF Collaboration)

[1] *Argonne National Laboratory, Argonne, Illinois 60439*
[2] *Istituto Nazionale di Fisica Nucleare, University of Bologna, I-40126 Bologna, Italy*
[3] *Brandeis University, Waltham, Massachusetts 02254*
[4] *University of California at Los Angeles, Los Angeles, California 90024*
[5] *University of Chicago, Chicago, Illinois 60637*
[6] *Duke University, Durham, North Carolina 27708*
[7] *Fermi National Accelerator Laboratory, Batavia, Illinois 60510*
[8] *Laboratori Nazionali di Frascati, Istituto Nazionale di Fisica Nucleare, I-00044 Frascati, Italy*
[9] *Harvard University, Cambridge, Massachusetts 02138*
[10] *Hiroshima University, Higashi-Hiroshima 724, Japan*
[11] *University of Illinois, Urbana, Illinois 61801*
[12] *Institute of Particle Physics, McGill University, Montreal H3A 2T8, and University of Toronto, Toronto M5S 1A7, Canada*
[13] *The Johns Hopkins University, Baltimore, Maryland 21218*
[14] *National Laboratory for High Energy Physics (KEK), Tsukuba, Ibaraki 305, Japan*
[15] *Lawrence Berkeley Laboratory, Berkeley, California 94720*
[16] *Massachusetts Institute of Technology, Cambridge, Massachusetts 02139*
[17] *University of Michigan, Ann Arbor, Michigan 48109*
[18] *Michigan State University, East Lansing, Michigan 48824*
[19] *University of New Mexico, Albuquerque, New Mexico 87131*
[20] *Osaka City University, Osaka 588, Japan*
[21] *Universita di Padova, Istituto Nazionale di Fisica Nucleare, Sezione di Padova, I-35131 Padova, Italy*
[22] *University of Pennsylvania, Philadelphia, Pennsylvania 19104*
[23] *University of Pittsburgh, Pittsburgh, Pennsylvania 15260*
[24] *Istituto Nazionale di Fisica Nucleare, University and Scuola Normale Superiore of Pisa, I-56100 Pisa, Italy*
[25] *Purdue University, West Lafayette, Indiana 47907*
[26] *University of Rochester, Rochester, New York 14627*
[27] *Rockefeller University, New York, New York 10021*
[28] *Rutgers University, Piscataway, New Jersey 08854*
[29] *Academia Sinica, Taipei, Taiwan 11529, Republic of China*
[30] *Texas A&M University, College Station, Texas 77843*
[31] *Texas Tech University, Lubbock, Texas 79409*
[32] *University of Tsukuba, Tsukuba, Ibaraki 305, Japan*
[33] *Tufts University, Medford, Massachusetts 02155*
[34] *University of Wisconsin, Madison, Wisconsin 53706*
[35] *Yale University, New Haven, Connecticut 06511*

Abstract

We present a measurement of the forward-backward charge asymmetry of the process $p\bar{p} \rightarrow Z^0/\gamma + X$, $Z^0/\gamma \rightarrow e^+e^-$ at $\mathrm{M}_{ee} > \mathrm{M}_Z$, using 110 pb^{-1}

of data at $\sqrt{s}$ = 1.8 TeV collected at the Collider Detector at Fermilab. The measured charge asymmetries are 0.43 ± 0.10 in the invariant mass region M_{ee} > 105 GeV/c^2, and 0.070 ± 0.016 in the region 75 GeV/c^2 < M_{ee} < 105 GeV/c^2. These results are consistent with the Standard Model values of 0.528 ± 0.009 and 0.052 ± 0.002, respectively.

PACS numbers: 13.38.+c, 12.15.Mm

The presence of both vector and axial-vector couplings in the process $q\bar{q} \rightarrow Z^0/\gamma \rightarrow e^+e^-$ gives rise to an asymmetry in the emission angle of the electron in the rest frame of the electron-positron pair, an effect which has been observed in previous hadron collider experiments [1]. To lowest order in the couplings, the angular differential cross section in the rest frame of the e^+e^- pair takes the form $\frac{d\sigma}{d(\cos\theta^*)} = A(1+\cos^2\theta^*) + B\cos\theta^*$, where θ^* is the emission angle of the e^- relative to the q momentum in the rest frame of the e^+e^- pair, and A and B are functions dependent on the weak isospin and charge of the incoming quarks and the electron pair invariant mass, M_{ee}. Extensions to this calculation which account for the proton structure [2], QED radiative effects [3], and leading order QCD effects [4] lead to a differential cross section of the same form. The forward-backward asymmetry in $\cos\theta^*$, A_{FB}, is a direct probe of the relative strengths of the vector and axial-vector couplings over the range of M_{ee} being considered. In addition, A_{FB} constrains the properties of any additional neutral gauge bosons not included in the Standard Model of electroweak interactions, in a way that is complementary to a direct search for excesses in the total cross section [5]. For values of M_{ee} significantly larger than M_Z, A_{FB} is predicted to be large and positive (near 0.5), so statistically significant deviations from the Standard Model can be observed with only a small number of events.

We present results using 110 pb^{-1} of data from proton-antiproton collisions with $\sqrt{s}$ = 1.8 TeV collected at the Collider Detector at Fermilab (CDF) during the 1992-1993 and 1994-1995 runs of the Fermilab Tevatron. CDF is described in detail elsewhere [6]. We briefly describe those aspects of the detector relevant to this analysis. The magnetic spectrometer consists of tracking devices inside a 3-m diameter, 5-m long superconducting solenoidal magnet which operates at 1.4 T. A set of vertex time projection chambers (VTX), which provide r-z tracking, are used to find the z position of the event vertex. Outside the VTX is the central tracking chamber (CTC), a 3.2-m long drift chamber used to measure charged particle momentum. The calorimeter is divided into a central barrel (pseudorapidity $|\eta| < 1.1$), and end-plugs ($1.1 < |\eta| < 2.4$), both of which are segmented into projective electromagnetic and hadronic towers [6]. The towers subtend approximately 0.1 in η by 15° in ϕ (central) or 5° in ϕ (end-plug). The energies of electrons are measured in the central electromagnetic calorimeter (CEM) and/or the end-plug electromagnetic calorimeter (PEM). The event vertex position and the position of the electromagnetic energy clusters in the calorimeters determine the 4-vectors of the electrons, which determine

$\cos\theta^*$ up to a sign. The charge of at least one of the electrons, obtained from a CTC track matched with an electromagnetic energy cluster, resolves the sign ambiguity.

We select a sample of events for which there exists at least one isolated CEM cluster with transverse energy $E_T > 20$ GeV, which also satisfies tight electron identification requirements; and at least one other isolated cluster in the CEM (PEM), with $E_T > 20$ GeV (15 GeV), and which satisfies looser requirements. The selection criteria are similar to those used in previous CDF analyses [7]. In addition, we require that the invariant mass of the two calorimeter clusters (M_{ee}) falls into one of two regions: a pole region (75 GeV/c^2 $< M_{ee} <$ 105 GeV/c^2) or a high mass region ($M_{ee} >$ 105 GeV/c^2). The two invariant mass regions were chosen in order to limit the sensitivity of A_{FB} to the absolute energy scale and to simultaneously minimize the statistical uncertainty of A_{FB} in each region. The events in each region are partitioned into a set where both electrons are found in the CEM (CC), and a set where the tight electron is found in the CEM and the loose electron is found in the PEM (CP). After applying all cuts, we find 98 CC events and 85 CP events in the high mass region, and 2602 CC events and 2861 CP events in the pole region. Figure 1 shows the distribution of invariant mass for the combined sample in each invariant mass region, as well as the relative number of forward and backward events in the samples. For each event, $\cos\theta^*$ is determined in the Collins-Soper frame [8], which reduces the uncertainty in $\cos\theta^*$ introduced by the transverse momentum of the incoming partons to a negligible level.

There are two important sources of background to the process $p\bar{p} \to Z^0/\gamma + X$, $Z^0/\gamma \to e^+e^-$: QCD dijet production, where both jets either contain or fake an electron; and electroweak processes (WW, WZ production, $t\bar{t}$ decay, and $Z^0 \to \tau^+\tau^-$) that produce two electrons in the final state. The number of background events due to dijets is determined from the asymmetry data sample by examining the number of same-sign (e^+e^+ or e^-e^-) events in each invariant mass region. The distribution in $\cos\theta^*$ for these events is obtained from a separate sample of QCD dijet events with kinematics similar to the asymmetry data [9]. In the high mass region, for CC events, every event has the charges of both electrons measured, and none of them are same-sign events. Thus there are 0^{+2}_{-0} QCD background events in the CC sample. In the high mass region, for CP events, the CTC can efficiently determine the sign of electrons in the PEM for tracks with $1.1 < |\eta| < 1.5$. None of these are same-sign events. The dijet sample is used to extrapolate the number of background events with $1.1 < |\eta| < 1.5$ into the entire fiducial region of the PEM. This extrapolation gives 0^{+21}_{-0} total QCD background events in the CP sample. In the pole region, similar calculations yield 0^{+2}_{-0} background events for CC events, and 110 ± 36 background events for CP events. Backgrounds due to other electroweak decay processes are determined from Monte Carlo calculations using PYTHIA [10] as an event generator. A fast detector simulation determines fiducial and kinematic acceptance of a particular event. For the CC and CP samples of the high mass region, there is estimated to be 1 electroweak background event in each. This background in the pole region is

insignificant.

Finite resolution in M_{ee} causes cross-contamination of events in the two invariant mass regions, thereby inducing systematic shifts in A_{FB}. The deconvolution of events in the two invariant mass regions is performed with a Monte Carlo calculation. We generate events using PYTHIA with MRSA [11] structure functions, and determine the amount of cross-contamination as a function of $\cos\theta^*$ via a fast detector simulation. The kinematic and geometric acceptance of an event is determined by the generated event topology and the known energy resolutions of the CEM and PEM. Identification of an accepted electron is determined from the CEM and PEM efficiencies, which were measured from CDF data in a way analogous to those of previous CDF analyses [7]. Mass deconvolution leads to corrections in A_{FB} of $+0.07 \pm 0.03$ in the high mass region and -0.010 ± 0.003 in the pole region. The uncertainty in A_{FB} induced by uncertainties in the absolute energy scales of the CEM and PEM is negligible.

We correct for electron identification efficiency and detector acceptance in each invariant mass region with the same Monte Carlo calculations used for mass deconvolution. We determine the ratio of background subtracted, mass deconvolved events generated, which pass our selection criteria, to the total number of events generated as a function of $\cos\theta^*$. The distribution in $\cos\theta^*$ of the data after background subtraction and mass deconvolution divided by this function gives the differential cross section for the process $p\bar{p} \to Z^0/\gamma + X$, $Z^0/\gamma \to e^+e^-$ up to a normalization factor. Figure 2 shows the resulting distributions of events for the two invariant mass regions. The region $|\cos\theta^*| > 0.8$ has very low acceptance and is excluded from consideration.

In order to extract the measured value of A_{FB}, we calculate its mean value for an ensemble of calculations wherein the data, the background, and the mass deconvolution corrections are all allowed to fluctuate about their mean values on a bin-by-bin basis in $\cos\theta^*$. Each raw data bin is allowed to fluctuate with a Poisson distribution. The total background level is allowed to fluctuate with a Gaussian distribution about its mean value. Background is subtracted from the raw data for a randomly varying set of values of $\cos\theta^*$, with a mean relative distribution determined by the QCD dijet sample. The distributions in $\cos\theta^*$ used to generate the mass deconvolution corrections are also allowed to fluctuate with a Poisson distribution in each bin. The mass deconvolution and efficiency corrections are then applied to give a differential cross section, from which an asymmetry value is calculated over the range $|\cos\theta^*| < 0.8$. We extrapolate this asymmetry value to the one which we would observe over the full range of $\cos\theta^*$ assuming a differential cross section of the form $A(1+\cos^2\theta^*) + B\cos\theta^*$. The quoted measurement of A_{FB} is the mean of this extrapolated asymmetry value for 100,000 such trial calculations. The uncertainty in A_{FB} is determined from the standard deviation in the distribution of A_{FB} in the ensemble.

Table I summarizes the measured values for A_{FB}. In the region defined by $M_{ee} > 105$ GeV/c^2, we measure A_{FB} to be 0.43 ± 0.08 (stat) ± 0.06 (syst) using a

	Pole Region		High Mass Region	
	CC	CP	CC	CP
Raw event sample	2602	2861	98	85
Forward events	1390	1513	56	75
Backward events	1212	1348	42	10
Background	0^{+2}_{-0}	110 ± 36	1^{+2}_{-1}	1^{+21}_{-1}
Predicted A_{FB}	0.052 ± 0.002		0.528 ± 0.009	
Measured A_{FB}	0.070 ± 0.016		0.43 ± 0.10	
Uncertainties in A_{FB}				
Statistical	0.015		0.08	
Background	0.002		0.04	
Mass Deconvolution	0.003		0.03	
Total uncertainty	0.016		0.10	

Table I: Experimental results for A_{FB}. There exist correlations between the different sources of uncertainty.

sample of 183 events. In the region 75 GeV/c^2 $< M_{ee} <$ 105 GeV/c^2, we measure A_{FB} to be 0.070 ± 0.015 (stat) ± 0.004 (syst) using a sample of 5463 events. Figure 3 compares the measurements with a Standard Model calculation [3], which includes QED radiative corrections, and assumes the MRSA structure functions and the PDG world average for $\sin^2 \theta_W^{eff}$ [12]. The measurements are consistent with the predictions of 0.528 ± 0.009 in the high mass region and 0.052 ± 0.002 in the pole region.

Models of additional heavy neutral gauge bosons predict large negative values for A_{FB} when M_{ee} is comparable to the boson's mass [5]. The accumulation of higher statistics of electron pairs in an invariant mass region above 350 GeV/c^2 [13], for example, would show significant downward deviations from the Standard Model prediction for A_{FB} in the presence of a heavy neutral gauge boson with a mass of 500 GeV/c^2 [14]. Although the statistics in this region are insufficient at present, measurements of A_{FB} in this region will provide a particularly strong test of the electroweak theory at very large M_{ee} in the future.

We thank the Fermilab staff and the technical staffs of the participating institutions for their contributions. We also thank U. Baur, for his help regarding the effect of radiative corrections on A_{FB}, and J. L. Rosner, for many useful discussions which helped motivate these measurements, and for his calculation of the effects of additional heavy neutral bosons on A_{FB}. This work was supported by the U.S. Department of Energy and National Science Foundation; the Italian Istituto Nazionale di Fisica Nucleare; the Ministry of Education, Science, and Culture of Japan; the Natural Sciences and Engineering Research Council of Canada; the National Science Council of the Republic of China; and the A. P. Sloan Foundation.

References

[1] F. Abe *et al.*, Phys. Rev. Lett. **67**, 1502 (1991);
P. J. Hurst, Ph.D. thesis, University of Illinois at Urbana-Champaign, 1990;
UA1 Collaboration, C. Albajar *et al.*, Z. Phys. C **44**, 15 (1989).

[2] J. L. Rosner, Phys. Lett. B **221**, 85 (1989).

[3] U. Baur (private communication).

[4] D. J. E. Callaway, Ann. Phys. **144**, 282 (1982); Phys. Lett. B **108**, 421 (1982).

[5] J. L. Rosner, Fermilab Report No. FERMILAB-PUB-95/394-T.

[6] F. Abe *et al.*, Nucl. Instrum. Methods Phys. Res., Sect. A **271**, 387 (1988). The CDF coordinate system defines r, ϕ, and z as cylindrical coordinates, with the z-axis along the direction of the proton beam. The angle θ is the polar angle relative to the z-axis, the pseudorapidity $\eta = -\ln(\tan(\theta/2))$, and the transverse energy $E_T = E\sin\theta$.

[7] F. Abe *et al.*, Phys. Rev. D **50**, 2966 (1995). We deviate from the cuts used in this reference, in that we do not require the tight central electron to trigger the event, and we relinquish the E/p cut for electrons with very stiff tracks (transverse momentum > 30 GeV/c).

[8] J. Collins and D. Soper, Phys. Rev. D **16**, 2219 (1977).

[9] For the QCD dijet sample, we require a tight electron in the CEM, no other isolated electromagnetic energy clusters in the event, low missing transverse energy, and an energetic hadronic jet. We calculate $\cos\theta^*$ by using the hadronic jet 4-vector in the place of an opposite-sign electron 4-vector.

[10] T. Sjöstrand, Comput. Phys. Commun. **82**, 74 (1994).

[11] A.D. Martin, R.G. Roberts and W.J. Stirling, Phys. Rev. D **50**, 6734 (1994).

[12] L. Montanet *et al.* (PDG), *Review of Particle Properties*, Phys. Rev. D **50**, (1994).

[13] There are two events observed in this region, with masses of 350 GeV/c^2 and 504 GeV/c^2, and with $\cos\theta^*$ of -0.14 and -0.27, respectively.

[14] CDF has previously measured the lower bound of the mass of a Z′ with Standard Model couplings to be 505 GeV/c^2. F. Abe *et al.*, Phys. Rev. D **51**, 949 (1995).

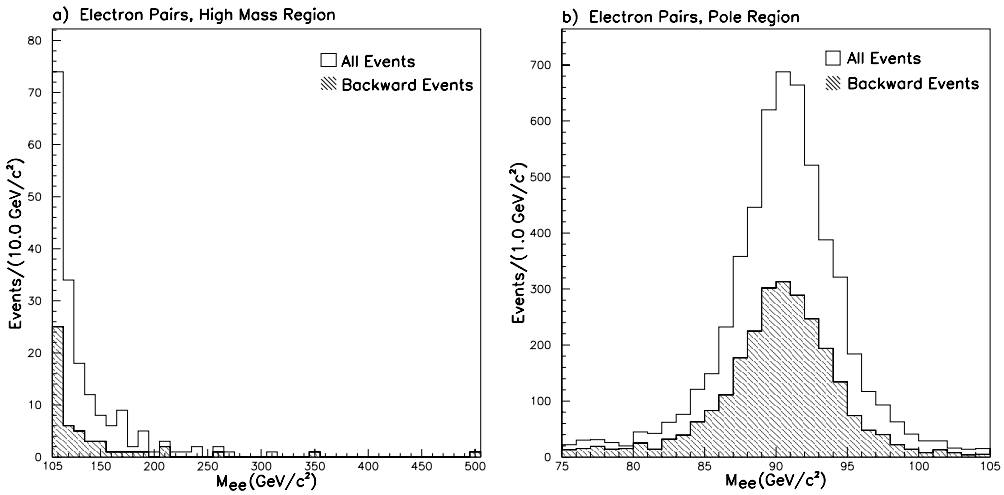

Figure 1: (a) The invariant mass distribution of events in the high mass sample. (b) The invariant mass distribution of events in the pole region sample.

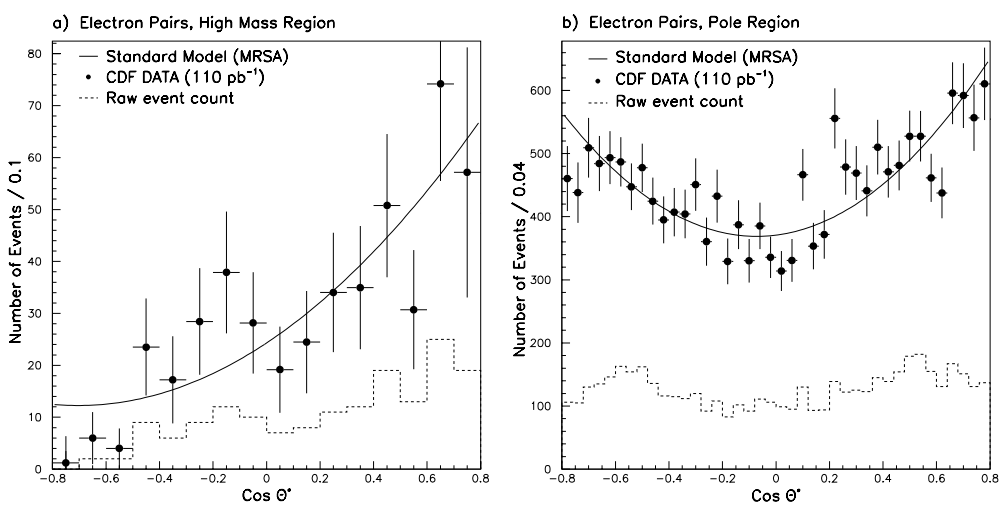

Figure 2: (a) The fully corrected distribution in $\cos\theta^*$ for events in the high mass region. The points are data after all corrections have been applied. The solid line is a Standard Model (MRSA) calculation, assuming the same normalization as the data. The dashed line is the raw number of events observed in our sample. (b) The same distribution for events in the pole region.

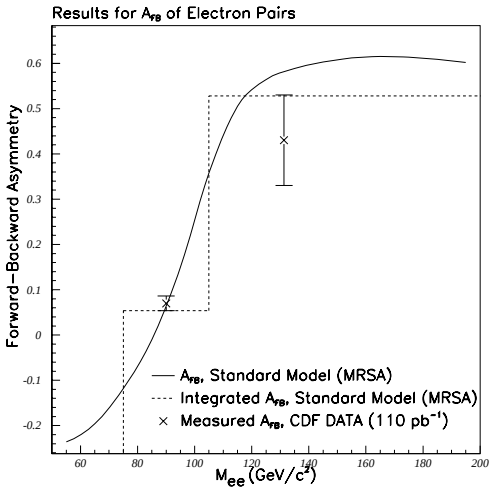

Figure 3: Results of our measurement of A_{FB}, compared with a Standard Model calculation. The solid line is a bin-by-bin Standard Model (MRSA) calculation of A_{FB}, and the dashed line is the same calculation integrated over the two mass regions in our analysis. The crosses are the experimental results for A_{FB} integrated over the same mass regions.